

Digital wavelength switching by thermal and carrier injection effects in V-coupled cavity semiconductor laser

Jialiang Jin (金嘉亮), Lei Wang (王磊), and Jianjun He (何建军)*

State Key Laboratory of Modern Optical Instrumentation, Center for Integrated Optoelectronics,
Department of Optical Engineering, Zhejiang University, Hangzhou 310027, China

*Corresponding author: jjhe@zju.edu.cn

Received March 30, 2012; accepted April 26, 2012; posted online August 3, 2012

Consecutive wavelength switching characteristics of a simple, compact, and digitally wavelength-switchable laser based on V-coupled cavities are reported. Wavelength switching through thermal and carrier injection effects is examined. Without using band gap engineering for the tuning section, 26- and 9-channel wavelength switching schemes are achieved via thermal and carrier injection effects, respectively. The performances of these two tuning schemes are then compared.

OCIS codes: 250.5960, 230.4555, 140.5960.

doi: 10.3788/COL201210.102501.

A wide wavelength tuning range is an important parameter for semiconductor lasers in advanced wavelength-division multiplexing (WDM) systems. As the WDM technology extends towards metro and access networks, cost reduction and operational simplicity become increasingly important. Unlike tunable lasers based on Bragg gratings^[1,2] or microelectromechanical system switches^[3], a recently proposed discrete wavelength-switchable V-coupled cavity laser does not require complex gratings, multiple epitaxial growths, or complex tuning algorithms^[4] while providing a wide wavelength tuning range and an excellent side-mode-suppression ratio (SMSR) near 40 dB^[5].

In this letter, the experimental results of the wavelength switching characteristics of the V-coupled cavity laser under thermal tuning are reported under a carrier injection scheme. We show that a maximum discrete 26-channel wavelength switching scheme with 100-GHz channel spacing and a SMSR of approximately 37 dB can be achieved using thermal effects via single-electrode control. Meanwhile, through carrier injection tuning, a nine-channel switching scheme with the same 100-GHz spacing and SMSR of approximately 32 dB was achieved without using any band gap engineering for the tuning section. With the potentially higher switching speed provided by the carrier injection, the V-coupled cavity laser can be used in advanced optical networks where the wavelength switching speed is crucial.

The V-coupled cavity laser was composed of a reflective 2×2 half-wave coupler and two waveguides with slightly different lengths. The etched facet version of the device is shown in Fig. 1(a). Three deep-etched facets define the reflecting mirror of the coupler and the other ends of the two resonant cavities. The fixed gain cavity (also referred to as short cavity) was designed to be 466- μm long so that its resonance frequency interval matches the 100-GHz spacing of the International Telecommunication Union operating frequency grid. As shown in Fig. 1(b), the channel selector cavity (long cavity) has a slightly different lengths (5%–10% length difference with respect to the fixed gain cavity) so that the Vernier effect can be used to increase the wavelength

switching range. The half-wave coupler where the cross-coupling coefficient has a relative phase of π with respect to the bar-coupling coefficient is essential for achieving high SMSRs^[6]. As shown in Ref. [4], the V-coupler has optimal coupling coefficients in amplitude and phase at the same time. Thus, its performance is superior to that of the previously reported Y-branch laser^[7]. Two electrodes covered the rear halves of the two cavities to be used for fixed gain and wavelength switching, and a joint electrode covered the front halves of the two cavities and the coupler region to provide a stable gain during operation. The laser was fabricated using a standard ridge waveguide InGaAsP/InP multiple quantum well (MQW) structure with five compressively strained 6 nm $\text{In}_{0.8}\text{Ga}_{0.2}\text{As}_{0.8}\text{P}_{0.2}$ quantum wells (QWs) sandwiched between 10-nm $\text{In}_{0.71}\text{Ga}_{0.29}\text{As}_{0.54}\text{P}_{0.46}$ barriers having photoluminescence peak wavelengths of approximately 1520 nm. The three facets were deeply etched to a depth of approximately 4 μm into the QW region via inductively coupled plasma (ICP) dry etching.

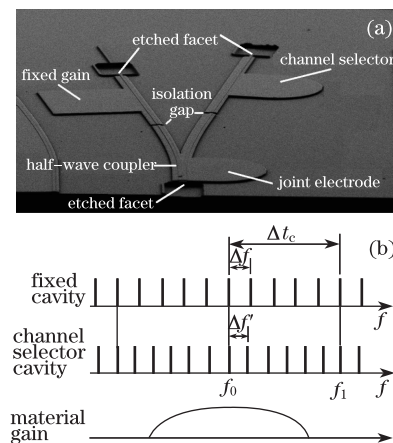


Fig. 1. (a) Scanning electron microscopy (SEM) image of the V-coupled cavity laser and (b) schematic diagram of the relationships between the resonant frequency combs of the two cavities during the digital wavelength switching via the Vernier effect.

All of the three sections under different electrodes constituted the same MQW structure without epitaxial re-growth or band gap engineering; thus, the fabrication complexity was substantially reduced. The total size of the device was about 500×300 (μm).

The device under test was mounted on an aluminum nitride chip carrier with a thermoelectric cooler controlled at 20°C . The laser reached the lasing threshold when all three electrodes were biased at about 20 mA. The LIV curves for single rear electrode tuning are shown in Fig. 2(a). With a turn-on voltage of approximately 0.8 V, the output power was measured by collecting light using a multimode fiber. Wavelength switching was achieved by varying the current injected into the long- or short-cavity electrode. This variation induced a refractive index change through either the thermo-optic or carrier injection effect. First, we tested the device for wavelength switching using the thermo-optic effect. When the currents injected into both cavities were above the threshold, the carrier density in the cavity remained almost constant with increasing current because of the clamping effect of the carrier density. Thus, the carrier-induced refractive index change was very small, and the thermal effect dominated the tuning mechanism. When we changed the current on one of the rear electrodes, the aligned peak in Fig. 1(b) shifted to an adjacent channel and so did the lasing wavelength. The switching directions were opposite when the current on either rear electrodes was increased. The refractive index increases with temperature but decreases with carrier density. Therefore, the switching directions of the thermal and carrier injection tuning schemes will also be opposite. Table 1 shows the relationship that can be deduced from the Vernier effect in Fig. 1(b). The gain spectrum shifted to a longer wavelength with increasing temperature and current; hence, we obtained more switching channels when we increased the current on the channel selector electrode on the long cavity. In this case, the wavelength switching was in the same direction as the material gain spectrum shift.

We tested two devices with 5% and 10% cavity length differences using the thermal tuning effect. Figure 2(b) shows the wavelength switching spectra for the device with 10% cavity length difference. The fixed gain and joint electrodes were biased at fixed current values of 22 and 46 mA, respectively. As the current on the channel selector electrode was increased from 22 to 135 mA, the lasing wavelength was switched over 16 channels with an SMSR of up to 40 dB.

The number of consecutively switchable channels can be further increased by reducing the cavity length differences and compromising the SMSR of the adjacent modes. For the device with 5% cavity length difference, Fig. 2(c) shows the 26 channels when the channel selec-

tor electrode was used tuned, whereas Fig. 2(d) shows the 14 channels when the fixed gain electrode was used. In Fig. 2(c), the channel selector electrode was tuned from 22.5 to 119.0 mA and the fixed gain electrode was biased at a fixed current of 34 mA. In Fig. 2(d), the short cavity electrode was tuned from 55 to 104.2 mA and the long cavity electrode was biased at 50 mA. In both cases, the joint electrode on the coupler was biased at 53 mA. The highest SMSR for this device was 37 dB, which is 3 dB lower than that of the device with 10% cavity length difference. This result is consistent with the theoretical prediction in Ref. [4].

In thermal tuning, we can achieve stable single-electrode tuning while the other two electrodes are biased with constant currents. The output power measured by collecting all light from the coupler side using a broad area detector was about 8 mW.

For the device with 5% cavity length difference, by design, the total range of switchable channels after the Vernier effect enhancement was about 16 nm, i.e., 20 channels, which can be obtained from

$$\begin{cases} \lambda_{\text{range}} = \sigma_{\text{enhanced}} \frac{\lambda_{\text{central}}^2}{2n_g L_{\text{fixed}}} \\ \sigma_{\text{enhanced}} = \frac{\Delta f}{|\Delta f - \Delta f'|} \end{cases}, \quad (1)$$

where σ_{enhanced} is the tuning enhancement information provided by the Vernier effect, Δf and $\Delta f'$ are the channel spacings of the two cavities, n_g is the group index of the waveguide, L_{fixed} is the length of the fixed gain cavity (short cavity), and λ_{central} is the central operating wavelength. Based on the experimental results, six extra switching channels were obtained when the switching direction was towards the longer wavelength. This result was obtained because of the material gain spectrum shift induced by the thermal effect^[8]. If the tuning was towards the shorter wavelength, the tuning range would be reduced by six channels, i.e., only 14 channels can be switched because the switching direction is opposite to the material gain spectrum shift (Fig. 2(e)).

Given that the material gain spectrum shift by the thermal effect was about 5 nm and the temperature coefficient was approximately 0.5 nm/K ^[8], the estimated junction temperature variation was approximately 10°C , which is relatively small. The thermal tuning scheme in this device did not require on-chip tuning resistors as in previously reported methods^[9,10]. Therefore, because of the large reverse current required on those resistors, the fabrication complexities were reduced and device damage was prevented. However, the operating current on

Table 1. Wavelength Switching Direction of the Two Tuning Schemes

Thermal Tuning		Carrier Injection		
Current Increase	Refractive Index Change	Switching Direction	Refractive Index Change	Switching Direction
Long Cavity	Increase	Longer Wavelength	Decrease	Shorter Wavelength
Short Cavity	Increase	Shorter Wavelength	Decrease	Longer Wavelength

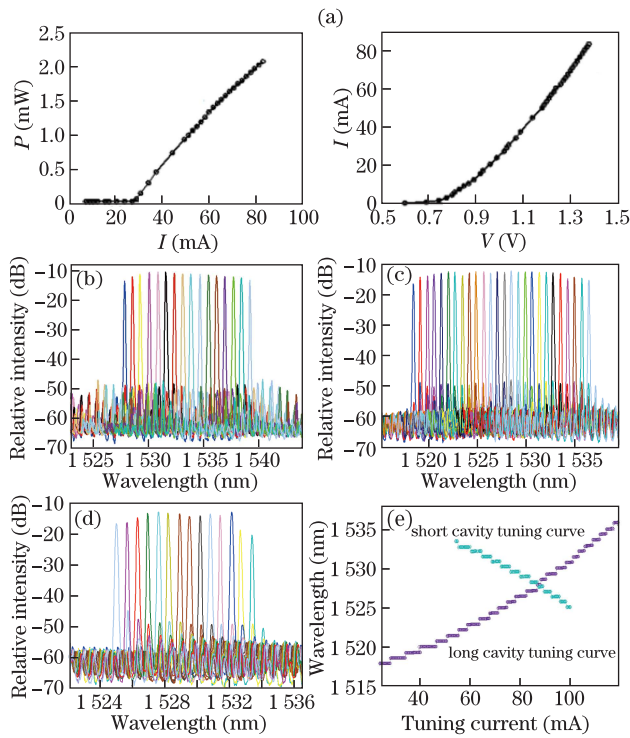


Fig. 2. (a) LI (left) and IV (right) curves for a single rear electrode; (b) 16-channel switching for the device with 10% cavity length difference when the current on the channel selector electrode is tuned using thermal effect; (c) 26-channel switching for the device with 5% cavity length difference when the current on the channel selector electrode in the long cavity is tuned; (d) 14-channel switching when the current on the fixed gain electrode in the short cavity is tuned; (e) plots of the wavelength versus tuning current for the device with 5% cavity length difference when the long or short cavity is tuned.

the tuning electrode almost reached 140 mA when the rightmost channel was selected. Therefore, power consumption and long-term stability became an issue. In addition, the channel switching speed under thermal tuning was in the millisecond range, which is not as fast as tuning by carrier injection (several nanoseconds). Hence, carrier injection must be employed to meet the requirements for applications such as optical burst and packet switching, in which the wavelength switching speed must be in the nanosecond range^[11].

We also studied wavelength switching by changing the carrier-induced refractive index. With current injection, the injected carriers caused a refractive index change because of the free-carrier plasma, band gap shrinkage, and band-filling effects^[12]. The overall result of these effects was a decrease in the refractive index of the waveguide. Ideally, refractive index tuning via carrier injection within a laser cavity should be conducted on a passive waveguide section with a band gap larger than that of the active waveguide producing the gain. This requirement can be met by using a band gap engineering technique such as QW intermixing or the etch-and-regrowth technique. However, this procedure was omitted in this letter to simplify the fabrication process. Consequently, the refractive index change in the tuning section due to carrier injection was very limited because of the carrier density clamping effect above the lasing threshold.

To maximize the carrier injection effect while minimizing the thermal effect, the tuning electrodes must be biased at a relatively low current. Therefore, the tuning section did not produce a significant gain, i.e., it was relatively passive in maximizing the carrier-induced refractive index change. The other two electrodes were biased with high currents to provide sufficient gain for the device to lase.

The SMSR of the all-active laser operated under this condition cannot be as high as that in the case of thermal tuning because of the imbalance of the operating current and gain in the two cavities. Theoretically, the SMSR is maximized by using equal round-trip gains for the two cavities^[4]. In this letter, we analyzed the case in which the round-trip gain for the two cavities is unequal. Figure 3 shows the threshold difference between the main mode and the highest side mode as a function of the normalized coupling coefficient (as defined in Ref. [4]) of the half-wave coupler for the cases of (a) equal round-trip gain ($gL = g'L'$), (b) equal gain ($g = g'$), (c) $g = g'/2$, and (d) $g = g'/3$, where g , g' and L , L' are the gain coefficients and cavity lengths for the short and long cavities, respectively. When the round-trip gains in the two cavities became increasingly unbalanced, the maximal threshold difference decreased and a lower SMSR was obtained.

Experimentally, when the channel selector electrode on the long cavity was tuned, the lasing wavelength switched towards the shorter wavelength with an increasing current. Figure 4(a) shows the measured switching spectra. When the current on the channel selector electrode was tuned from 0.36 to 10 mA, a switching of five consecutive channels was obtained. To maximize the SMSR, the current on the fixed gain electrode was adjusted from 64.6 to 36.2 mA while the current on the joint electrode was fixed at 51.22 mA. In this case, the highest SMSR was 31 dB.

On the other hand, when we tuned the electrode in the short cavity, the lasing wavelength switched towards the longer wavelength with an increasing current. We obtained nine consecutive channels when the tuning current was increased from 0.42 to 5.15 mA, as shown in Fig. 4(b). To maximize the SMSR, the current on the channel selector electrode was adjusted from 47.5 to 86.4 mA while the current on the joint electrode was fixed at 50.8 mA. The highest SMSR was 32 dB.

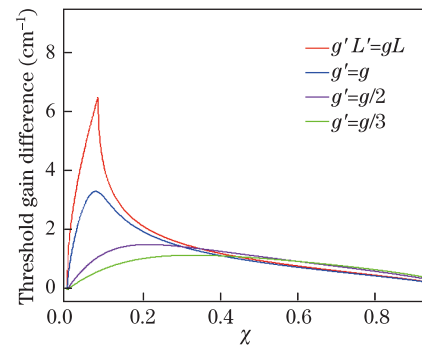


Fig. 3. Threshold difference between the main mode and the highest side mode as a function of the normalized cross-coupling coefficient under different gain relationships between the two cavities.

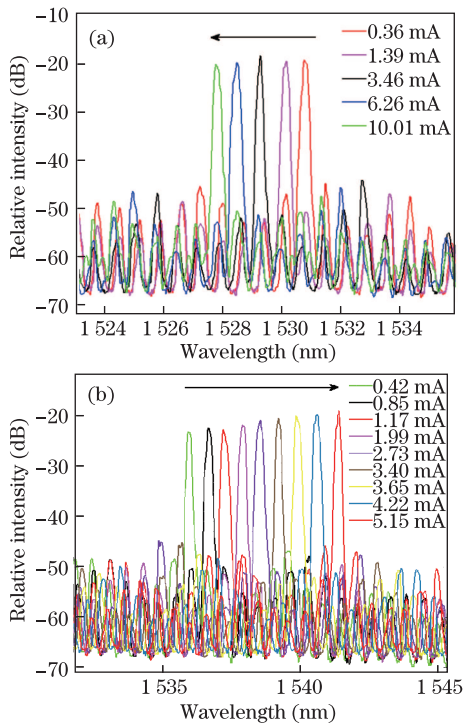


Fig. 4. (a) Switching of five consecutive channels when the electrode in the long cavity is tuned using the carrier injection effect; (b) switching of nine consecutive channels when the electrode in the short cavity is tuned using the carrier injection effect. The switching directions with increasing current are indicated.

Carrier injection is inevitably associated with a parasitic thermo-optic effect because it also causes the heating of the device. The wavelength shifts of the two effects exhibit different signs; hence, they compensate each other to a certain degree^[8]. When the tuning current is increased above a threshold value, the consecutive channel switching induced by the carrier injection effect stops as the thermal effect becomes dominant. When the current in the tuning electrode is tuned to switch the wavelength, the SMSR can be maximized by adjusting the current on the other cavity electrode and thus shift the material gain peak towards the operating wavelength through the thermal effect. As a result, the tuning range is larger when the wavelength switching direction is the same as that of the gain spectrum shift induced by thermal effect. To improve the SMSR and tuning range under the carrier injection regime, the laser is operated under the equal round-trip gain condition with the tuning section producing no gain. A band gap engineering technique must be employed to blue-shift the band gap of the tuning section. In this case, the tuning current would no longer influence the gain of the device, and the carrier clamping and parasitic thermal effect can also be reduced. QW intermixing^[13] is a promising technique for low-cost band

gap engineering and is currently in progress.

In conclusion, the discrete wavelength switching in V-coupled cavity laser based on thermal tuning and carrier injection effect is studied. The continuous switching of 26 channels with maximum SMSR of 37 dB is achieved using the thermal-optic effect. Without epitaxial regrowth or band gap engineering, the wavelength switching via carrier injection is demonstrated in the V-coupled cavity laser. The wavelength switching of nine consecutive channels with an SMSR of approximately 32 dB is achieved. Although the tuning range and the SMSR are not as high as those obtained via thermal tuning because of the limitations of the carrier clamping effect and unbalanced round-trip gain, the performance can be improved by introducing a band gap blueshift by using techniques such as QW intermixing.

This work was supported by the National Natural Science Foundation of China (No. 60788403) and the Natural Science Foundation of Zhejiang Province (No. Z1110276).

References

1. V. Jayaraman, A. Mathur, and L. A. Coldren, *IEEE J. Quantum Electron.* **29**, 1824 (1993).
2. A. J. Ward, D. J. Robbins, C. Busico, L. Ponnampalam, J. P. Duck, N. D. Whitbread, P. J. Williams, D. C. J. Reid, A. C. Carter, and M. J. Wale, *IEEE J. Select. Topics Quantum Electron.* **11**, 149 (2005).
3. B. Pezeshki, E. Vail, J. Kubicky, G. Yoffe, S. Zou, J. Heanue, P. Epp, S. Rishton, D. Ton, B. Faraji, M. Emanuel, X. Hong, M. Sherback, V. Agrawal, C. Chipman, and T. Razazan, *IEEE Photon. Technol. Lett.* **14**, 1457 (2002).
4. J.-J. He and D. Liu, *Opt. Express* **16**, 3896 (2008).
5. J. Jin, L. Wang, T. Yu, Y. Wang, and J. He, *Opt. Lett.* **36**, 4230 (2011).
6. X. Lin, D. Liu, and J.-J. He, *Appl. Opt.* **48**, F19 (2009).
7. M. Schilling, H. Schweitzer, K. Dutting, W. Idler, E. Kuhn, A. Nowitzki, and K. Wunstel, *Electron. Lett.* **26**, 243 (1990).
8. J. Buus, M. C. Amann, and D. J. Blumenthal, *Tunable Laser Diodes and Related Optical Sources* (Wiley-Interscience, New Jersey, 2005).
9. S. L. Woodward, U. Koren, B. I. Miller, M. G. Young, M. A. Newkirk, and C. A. Burrus, *IEEE Photon. Technol. Lett.* **4**, 1330 (1992).
10. M. Oberg, S. Nilsson, T. Klinga, and P. Ojala, *IEEE Photon. Technol. Lett.* **3**, 299 (1991).
11. L. Xu, H. G. Perros, and G. Rouskas, *IEEE Commun. Mag.* **39**, 136 (2001).
12. B. R. Bennett, R. A. Soref, and J. A. Del Alamo, *IEEE Photon. Technol. Lett.* **26**, 113(1990).
13. J. J. Dubowski, C. N. Allen, and S. Fafard, *Appl. Phys. Lett.* **77**, 3583 (2000).